fortune Journals

Research Article

ARCHIVES OF
CLINICAL AND
BIOMEDICAL RESEARCH

ISSN: 2572-5017

AURKA/NFκB Axis: A Key Determinant of Radioresistance in Cervical Squamous Carcinoma Cells

Salini Das[1], Dilip Kumar Ray[2], Elizabeth Mahapatra[1], Souvick Biswas[1], Debomita Sengupta[1], Madhumita Roy[1], Sutapa Mukherjee[1*]

Abstract

Cervical cancer being one of the leading gynecological cancers, poses a major threat by its ever-increasing trend of global recurrence. Radioresistance, one of the major challenges confronted during the treatment of cervical cancer is manifested by increased rate of cellular proliferation, migration, invasion and alterations in cell cycle. Aurora Kinase A (AURKA), a mitotic serine/threonine kinase was found to be overexpressed in cancers and is associated with development of acquired therapy resistance. The principal objective of this study was to explore the mechanisms by which AURKA confers radioadaptive response in cervical cancer cells. Parental cervical squamous carcinoma cell line SiHa was subjected to recurrent challenge towards fractionated dose of X-irradiation. Finally, a resistant subline (SiHa/RR) was isolated at 40Gy. SiHa/RR exhibited higher expression of AURKA/ pAURKA along with activation of the signaling pathways (HIF1α, pAkt, NFκB) vis-à-vis lower expressions of the proteins (p53, Gadd45a), which are generally suppressed by AURKA. Interestingly, inhibition of AURKA in SiHa/RR showed improved radiosensitivity by reducing cell viability, restrained wound healing capacity as well as sphere forming ability and accelerated radiation induced apoptosis. Ectopic overexpression of AURKA gave rise to radioresistant phenotype in parental SiHa by stimulating nuclear translocation of NFκB. This pattern of increased nuclear localization of NFκB was also observed in resistant subline as a consequence of activation and overexpression of AURKA. These findings strengthened the active involvement of AURKA in radioresistance via driving NFκB mediated signaling pathway to deliver radioresistant associated adaptive complexities.

Keywords: Acquired Radioresistance; AURKA; Cervical Squamous Carcinoma Cells; Prosurvival Signaling; Radioadaptive Response

Introduction

Cervical cancer prevails as one of the leading gynecological cancers for its higher incidences and mortality [1-3]. Therapeutic success might be achieved against cervical cancer at early stage of diagnosis, primarily by surgery or radiation [4, 5]. The metastatic form of carcinoma is yet a challenging regimen that seeks urgent attention to explore novel therapeutic approaches. Globally, cervical cancer has a moderate to high recurrence rate throughout the stages after the initial treatment because of survival of cancer cells which escapes radiation therapy and causes disease relapse [6, 7, 8]. Understanding the underlying strategies of these surviving cells is an urgent need of the hour. Most of the time, the efficacy of radiation therapy depends on the phases

Affiliation:

[1]Department of Environmental Carcinogenesis & Toxicology, Chittaranjan National Cancer Institute, 37, S. P. Mukherjee Road, Kolkata 700 026, India

[2]Department of Medical Physics, Chittaranjan National Cancer Institute, 37, S. P. Mukherjee Road, Kolkata 700 026, India

***Corresponding author:**
Sutapa Mukherjee, Department of Environmental Carcinogenesis & Toxicology, Chittaranjan National Cancer Institute, 37, S. P. Mukherjee Road, Kolkata 700 026, India.

Citation: Salini Das, Dilip Kumar Ray, Elizabeth Mahapatra, Souvick Biswas, Debomita Sengupta, Madhumita Roy, Sutapa Mukherjee. AURKA/NFκB Axis: A Key Determinant of Radioresistance in Cervical Squamous Carcinoma Cells. Archives of Clinical and Biomedical Research 6 (2022): 707-721.

Received: August 13, 2022
Accepted: August 22, 2022
Published: September 16, 2022

Das S et al., Arch Clin Biomed Res 2022
DOI:10.26502/acbr.50170282

of cell cycle. The relative radiosensitive response of a cell becomes highly active at the G2/M phase making the G2/M arrest the master strategy of radiation induced killing of cells [9, 10]. Alteration in the cell cycle pattern is therefore a key to achieve radioresistance [11,12]. Aurora Kinase A (AURKA) is an important mitotic serine threonine kinase, predominantly accountable for G2/M progression of cell cycle [13]. Conventionally AURKA promotes proper mitotic exit, stabilization of centrosome, formation of spindle as part of its canonical mitotic role [14]. Moreover, involvement of AURKA is also evident in the development of acquired chemoresistance in several cancers [15]. Radioresistance is predominantly caused by accumulation of altered adaptive characters within the cells which is manifested by reshaping the cellular behavior such as hyper proliferative capability, EMT phenotype and induction of stemness within them [16]. Previous researches proposed AURKA as a key contributor of radioresistance; yet the underlying mechanisms need elucidation [17,18]. Therefore, understanding AURKA mediated signaling pathway in radioresistant scenario may put forward opportunities for exposure of new domains of molecular therapy. The present study has been taken up to find out the actual adaptive features gained during chronic cumulative irradiation at the cellular level. Attempts were undertaken to develop and characterize radioresistant cervical cancer cell line via fractionated irradiation. Successive molecular assays were carried out in order to explore and establish the demand of AURKA in acquiring cellular adaptability for imparting radioresistance; where NFκB mediated activation of prosurvival pathway was found to be favored by AURKA.

Materials and Methods

Chemical Reagents

Procurement of the necessary primary antibodies like anti-HIF1α, anti-p53, anti-Akt, anti-phospho-Akt (S473), anti-FITC-conjugated anti-rabbit IgG was done from Genetex, CA, USA. Anti AURKA and anti-pAURKA(T288) were purchased from Cell Signaling Technology, MA, USA. β-actin antibody were procured from abcam, Cambridge, UK. Anti-NFκBp50, p65, anti-MMP9 and anti-Oct 4 antibodies were obtained from Santa Cruz, TX, USA. anti-Gadd45α was purchased from Elabscience, TX, USA. BSA (Bovine Serum Albumin), PI (Propidium Iodide), DAPI (4′,6 diamidino-2-phenylindole), Aurora-A Inhibitor I (AKI) were purchased from Sigma-Aldrich, Bangalore, India. All other reagents of analytical grade were procured locally.

Cell Lines and Cell Culture

SiHa, a human cervical squamous carcinoma cell line (HPV 16+, p53+, Rb+) was obtained from National Centre for Cell Science (NCCS), Pune India. A Radioresistant subline SiHa/RR was developed from parental SiHa by weekly incremental fractionated irradiation doses with an initial dose of 2 Gy followed by weekly incremental doses of 0.5 Gy. Cells were maintained in each irradiated dose for 5 passages. Finally a resistant colony was isolated at 40 Gy; designated as SiHa/RR. Both SiHa and SiHa/RR cells were maintained in MEM supplemented with 15% heat inactivated fetal bovine serum (FBS) and antibiotics (gentamycin 40 µg, penicillin 100 units, streptomycin 10µg/ml). Cells were maintained at 37^0C in a humidified CO_2 incubator having 5% CO_2/95% air.

Morphological Observation and Cell Viability Assay

Cellular morphological observation of SiHa and SiHa/RR cells was carried out under the inverted microscope (Olympus) at the magnification of 400X. Images were captured and analyzed (Nucleus: Cytoplasm) using FIJI software. The alterations in the ratio were plotted graphically. Roughly $1x10^5$ cells were seeded into a 25 cm^2 flask (Greiner Bio One International) 48 h prior to the first irradiation. These cells were weekly exposed to previously mentioned doses of X-Ray.

Estimation of Cell Viability by MTT Assay

Confirmation of acquired radioresistance was evaluated by the percentage of viable cells upon challenging with acute radiation dose in both SiHa and SiHa/RR. Cells at a number of 10000 per well was seeded in 96-well plate. After 24 h of incubation, both SiHa and SiHa/RR cells were irradiated with different doses (2, 4, 6, 8, 10Gy radiation). Estimation of viable cells were conducted upon treatment with MTT (4,5-Dimethylthiazol-2-yl)-2,5-Diphenyl tetrazolium Bromide) solution 50 µl (1.2 mg/ml in water). After 5h of incubation period required for the development of formazan products, cells were centrifuged at 1000 rpm for 5 min. The supernatant was discarded and volume was replenished using DMSO to dissolve MTT formazan product which gave rise to purple coloured solution. The optical density value of final products signifying viable cells was estimated in ELISA plate reader (TECAN) at an absorbance maximum of 570 nm. This set of experiment was furthermore repeated with pretreatment with a specific Aurora Kinase Inhibitor I or AKI (0.01µM for 24 h) prior to exposure to different radiation doses.

Flow Cytometric Analysis

To investigate the modification in the cell cycle phases between SiHa and SiHa/RR in the presence and absence of irradiation, flow cytometric analysis was performed necessarily. Initially, both the cells were seeded at an initial number ($2x10^6$) followed by exposure to 10Gy of acute X-irradiation. After 6h of treatment, cells were trypsinized, suspended in PBS for centrifugation at 1500 rpm for 8 min. Pellets were fixed in 70% cold absolute ethanol followed by incubation in ice for 30 min. Cells re-centrifuged for ethanol removal and pellets were suspended in 1ml DNA binding solution (200 µg/ml RNase + 50 µg/ml PI), kept in dark for

Das S et al., Arch Clin Biomed Res 2022
DOI:10.26502/acbr.50170282

30 min before analysis in BD Fortessa Flow Cytometer. Fluorescence was captured on FL2H channel and 10,000 cells with logarithmic amplification were counted. Analysis of flowcytometric data was perfornmed in BD FACSDIVA software.

Immunoblotting Technique

Immunoblotting technique was used to identify the level of expression of protein of interest by the standard laboratory protocol [19, 20]. Briefly, 6h post irradiated (10Gy) and untreated control cells were harvested and cell lysates were prepared using lysis buffer. In a separate set of experiments, SiHa/RR cells were pretreated with AKI (24h) followed by 10Gy irradiation and 6h post-incubated cells were harvested for lysate preparation. Estimation of protein concentration was obtained by the Bradford Colorimetric assay. Equal concentration of proteins was loaded in SDS-polyacrylamide gel and electrophoresis was performed using standard buffer (Tris: 25 mM, glycine: 192 mM, SDS: 20%) (Bio-Rad apparatus) and electro-transferred to nitrocellulose membranes using transfer buffer (Tris: 250 mM, glycine: 192 mM, methanol: 10%). Membranes were blocked in 5% BSA to avoid nonspecific binding of antibody. Membranes were then incubated overnight with respective primary antibodies at 4^0C. Following incubation, membranes were washed with TBST (Tris Buffered Saline with Tween-20) thrice and alkaline phosphatase-conjugated anti-mouse IgG or anti-rabbit IgG (1:1000 dilutions in TBS) was added to it. Membranes were washed after a brief incubation period with TBST for removal of nonspecific binding of secondary antibodies, prior to addition of BCIP/NBT to visualize the proteins in the form of colorimetric bands.

Immunofluorescence

Intracellular localization of the target proteins were detected by immunofluorescence technique. Seeding of $1x10^5$ cells was performed in 6 well plates on the coverslip. Cells were irradiated with or without AKI treatment (6h pretreatment) and were further post-incubated for another 6h. Thereafter, cells were rinsed twice with PBS followed by fixation in 2% paraformaldehyde in PBS for 10 min at RT. Cells were kept for 10 min at 4^0C in permeabilization buffer (0.5% Triton X-100 in PBS or PBST) afterwards followed by adequate washing with PBST. Blocking solution (PBST with 2% BSA) was then added to cells for proper blocking upto 30 min. Primary antibody (anti- Aurora Kinase A, NFκB p50/p65) was next added to the cells and were kept for 2 h at RT. Subsequent washing was done in PBST (PBS+0.1% Tween 20) for five times; 5 min each. Secondary antibody conjugated with fluorescein isothiocyanate (FITC) was added and kept additionally at 37^0C for 2 h. Following nuclear counterstaining with DAPI, cells were mounted on microscopic slides by DPX. Microscopic observation was done using a fluorescence microscope (Leica) at a magnification of 400X. Images were visualized and analyzed in Las X software.

In Silico Network Analysis

String Database was used to study the interactions between the proteins which were found to be overexpressed in SiHa/RR cells based on the formula Network analysis = Network Enrichment Analysis + Network Topological Analysis.

Ectopic Overexpression of AURKA Using Plasmid DNA

Confluent SiHa cells were added with specific plasmid with the modified pcDNA5/FRT/TO vector containing a single amino-terminal Myc tag and the human wild type AURKA transgene (Plasmid #59804; pcDNA5 FRT TO Myc ArA WT, AddGene) and lipofectamine to Opti-MEM aliquots (250 µl each) and incubated for 5 min at room temperature. Thereafter, plasmid/Opti-MEM and the Lipofectamine 3000/Opti-MEM was mixed and allowed to incubate for 20 min at RT. Plasmid containing medium was added to cells in culture. Finally, expression was checked by western blotting and immunofluorescence assay.

Detection of Apoptosis by TUNEL Assay

To examine the characteristic morphological features of apoptosis, both SiHa and SiHa/RR cells were exposed to acute shot of irradiation of 10Gy. Cells were harvested, 6h after irradiation, washed with PBS and were smeared in the glass slide coated with poly-L lysine. Thereafter 50 µL of the labeling reaction mixture (prepared as per information provided with the TaKaRa in situ Apoptosis Detection kit) (Catalogue no# MK500) was added to both the cells. The same protocol was applied to AKI pretreated cells (as described in earlier experimentations) as well. Cells were then incubated in the dark in humidified chamber at 37^0C for 90 min. Characteristic apoptotic cells were examined from the mounted slides at 400X magnification under a fluorescence microscope at specific filter (Leica).

In Vitro Wound Healing Assay

Alteration of cell motility was determined using in vitro scratch or migratory assay. The treatment conditions were a). Untreated SiHa and SiHa/RR cells, b). 6h post irradiated cells (10Gy acute shot) and c). Cells pretreated with AKI (0.01 µM) for 6h followed by 10Gy X-irradiation and subsequent incubation for another 6h. A scratch was drawn in a straight line over the monolayer of the confluent culture using 200µl sterile pipette tip. The image of the scratch width was captured under a phase-contrast microscope, immediately after treatment and again after 36h of incubation. Percentage of wound healing area was determined by calculating the reduction of the scratch-width (width of the space devoid of migrating cells) after the indicated incubation time and expressed as percentage of wound closure. Scratch area was calculated using FIJI software.

Das S et al., Arch Clin Biomed Res 2022
DOI:10.26502/acbr.50170282

Sphere Formation Assay

3D sphere forming assay was carried out using hanging drop method as described by Foty with slight modifications [21]. Treatment conditions were similar to that of wound healing assay. Following completion of treatment condition, cells were trypsinized and resuspended in the medium. The lid of a 60 mm tissue culture plate was removed and inverted to deposit 10 µl drops of cell suspension. Twenty (20) such drops were placed in well maintained distance from each drop. The lower plate was filled with 5 ml of sterile PBS to use it as a hydration chamber. The PBS-filled chamber was covered by the lid containing cell droplets. Such plates were kept for incubation at 37^0C/5% CO_2 with 95% humidity till visible cell sheets or aggregates were found on the lid. After microscopical confirmation of conspicuous cell sheets, those were transferred to 25 cm^2 flasks filled with 3 ml complete medium and were placed in shaker incubator at 37^0C and 5% CO_2 till the development of spheroids. Microscopic observation and capturing of image were performed at the 100X magnification using a phase contrast microscope (Zeiss). Further measurement of sphere area was performed using FIJI software.

Statistical Analysis

Comparative analysis of differences between groups was carried out using Student's t test in the GraphPad Prism 5.0 software package (GraphPad Software, Inc., La Jolla, CA, USA). $p<0.001$ was considered as the maximum level of significance. Data or values were obtained from at least three independent experiments and expressed as Mean ± SD.

Results

Confirmation and Characterization of Radioresistant Subline SiHa/RR

To perceive the role of AURKA in radioresistance, a radioresistant cervical squamous cell carcinoma cell line (SiHa/RR) was developed by subjecting parental SiHa cell to weekly fractionated dose of X-irradiation with an initial dose of 2Gy followed by a weekly incremental dose of 0.5 Gy. Finally, the subline was isolated at a cumulative dose of 40 Gy. Isolated radioresistant subline was further maintained at a steady state weekly radiation of 2 Gy. The morphological changes of SiHa/RR cells were examined under inverted microscope at the magnification 400X. Results exhibited enlarged nuclei in SiHa/RR cells with increased Nucleus to Cytoplasmic (N/C) ratio. N/C ratio as observed in SiHa (1:3) was found to increase significantly (4:1) in radioresistant SiHa/RR cells (Figure 1A and B). Since higher nucleo-cytoplasmic ratio is indicative towards proliferative potencies, attempts were made to look into the doubling time of SiHa/RR. Using the slope of log phased cells as plotted in the graph, it was noticed that the doubling time of parental SiHa was 33 h while that of SiHa/RR was shortened to 24 h; indicating enhanced proliferating potential upon acquirement of radioresistance (Figure 1C). Additionally, confirmation of radioresistance of SiHa/RR was assessed by MTT assay where nearly 50% cells of parental SiHa were killed upon treatment with 4 Gy radiations. Contrarily, SiHa/RR cells remained viable at 4Gy radiation and viability of SiHa/RR prevailed upto 50% even upon acute exposure dose of 10Gy (Figure 1D). This dose of radiation (10Gy) was used in the further experimentations to investigate the molecular basis of radioresistance. Presumptive indications of better survivability as depicted from the MTT results were further validated in the western blot analysis. Results depicted elevated expression of mitotic kinase AURKA and its activated form pAURKA(T288). Such an elevated expression of active form of AURKA substantiated the conviction of its contribution in development of radioresistant phenotype. HIF1α, a key orchestrator of radioresistance and an upstream regulator of AURKA was looked furthermore. Radiation induced HIF1α was clearly visible in SiHa, whereas a trend of overexpression pattern of the same was observed in SiHa/RR. Since activated AURKA phosphorylates Akt at Serine 473 residue, expression of Akt and phospho Akt were examined furthermore. The result showed surged expressions of total Akt, phospho Akt (S473) (Figure 1E). Expression status of DNA damage regulator proteins like p53, Gadd45α as well as (NFκB p50/65) which are the downstream effectors of Akt, were checked in both SiHa and SiHa/RR (Figure 1F). Downregulated expressions of p53, Gadd45α with corresponding upregulations of NFκB p50/65 enabled SiHa/RR cells to survive even after acute radiation exposure of 10Gy. Next it was felt interested to check whether any interactive association exists between these altered proteins as observed in SiHa/RR. String Database analysis was performed which indicated a prominent interactive relationship between AURKA, NF-κB, p53, Gadd45α, HIF1α. This *in silico* finding notified a possible signalling mechanism in SiHa/RR which favoured the phenotypic changes in SiHa/RR for acquirement of radioresistance (Figure 1G).

Elevated AURKA Level Protects Radioresistant Subline SiHa/RR from Radiation Induced G2/M Arrest

Elevated expression of AURKA was reassured from the immunofluorescence study of SiHa and SiHa/RR cells either untreated or irradiated with 10Gy radiation. Images were captured in the fluorescent microscope (Leica) at 400X magnification. The images depicted upregulated centrosomal as well as nuclear AURKA in SiHa/RR even after challenging with 10Gy irradiation (Figure 2A). Increased expression of AURKA in SiHa/RR made the investigators curious to check the alteration in the Cell cycle phase distribution between SiHa and SiHa/RR using flow cytometer (BD Fortessa). SiHa and SiHa/RR cells at 0 and 10Gy of acute radiation doses were harvested 6h after

Das S et al., Arch Clin Biomed Res 2022
DOI:10.26502/acbr.50170282

irradiation and finally stained with DNA binding solution containing propidium iodide. The result analysed at propidium iodide specific filter, displayed higher proportion of arrest of SiHa cells at G2 phase upon exposure to acute dose of 10Gy radiation. Conversely, SiHa/RR exhibited significantly lower proportion of cells at G2/M phase; even after same dose of exposure (Figure 2B). Graphical representation of phase wise distribution of cells (Figure 2C), indicated that SiHa/RR cells efficiently escaped from the radiation induced cell cycle arrest and led to significant ($p < 0.001$) progression towards M phase from G2 phase. Percentage values obtained were Mean ± SD of three independent experiments.

Ectopic Overexpression of AURKA Increases Radioresistance in Parental SiHa by Stimulating Nuclear Translocation of NF-κB

The striking upregulation of AURKA and its correlation of radioresistance in SiHa/RR cells encouraged to explore whether ectopic overexpression of AURKA in parental SiHa cells would result in similar radioresistant phenotype in SiHa as that of SiHa/RR. To achieve this goal, SiHa cells were transfected with AURKA plasmid. AURKA mediated tumor forming ability was assessed *in vitro* by sphere forming assay. AURKA overexpressed SiHa cells exhibited increased sphere area compared to control SiHa (Figure 3A). Overexpressions of AURKA along with its downstream target NFκB (p50/p65) were confirmed in SiHa cells by western blotting (Figure 3B). Immunofluorescence (IF) study also corroborated with the western blot results. Since a major difference in cell cycle was observed between SiHa and SiHa/RR particularly at the G2/M population, flow cytometric analysis of cell cycle was performed in parental SiHa as well as AURKA-overexpressed SiHa cells. The data revealed a

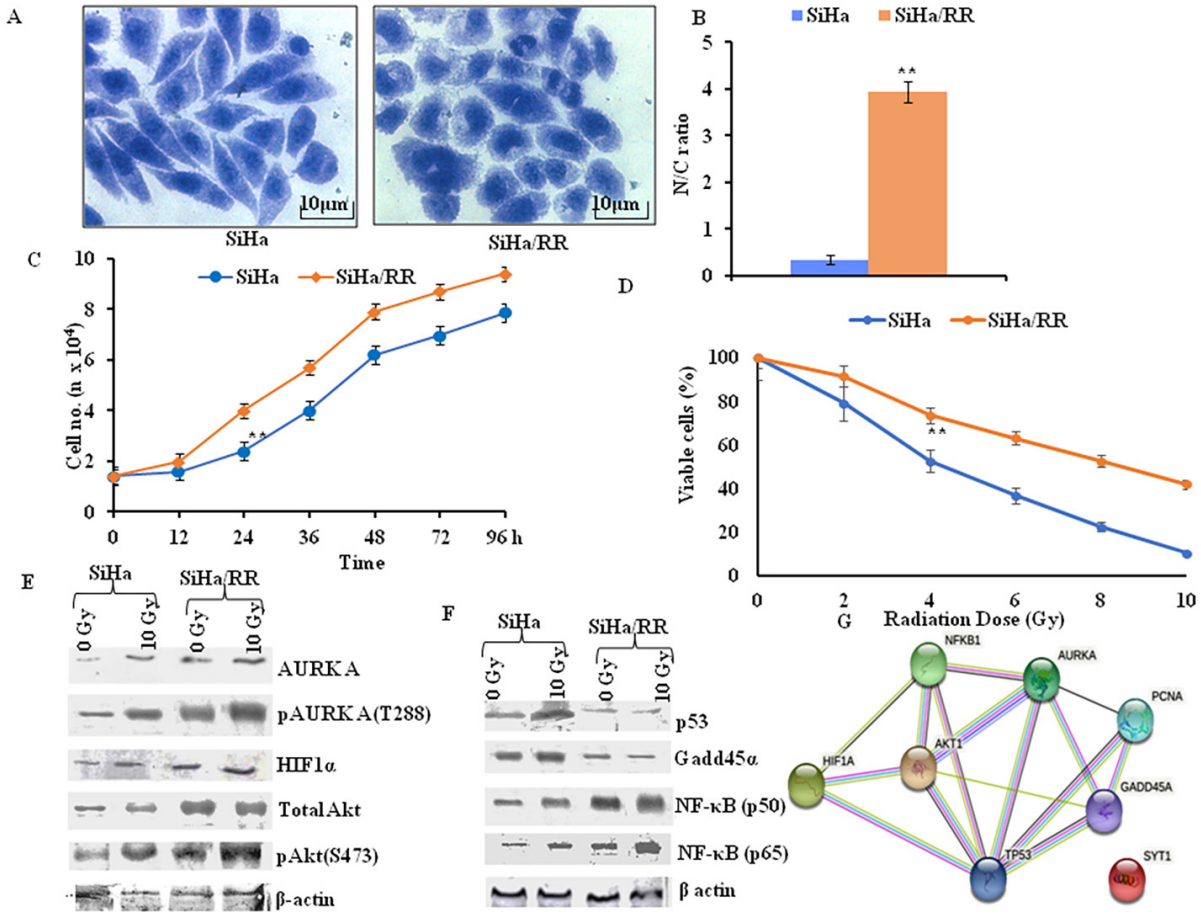

Figure 1: Characterization of acquired radioresistant phenotype in cervical squamous carcinoma cell line *in vitro*: A. Distinct morphological features of representative crystal violet stained SiHa and SiHa/RR as observed under Phase Contrast Microscope at 400X magnification; exhibited altered cellular morphology in SiHa/RR as opposed to SiHa. B. Corresponding Nucleus:Cytoplasm ratio was plotted. The values obtained are Mean ± SD of three independent experiments. Approx 150 – 200 cells were scored at a time C. Resistance to radiation of SiHa/RR was further verified by reduced doubling time. Equal numbers of cells were seeded and cell numbers were recalculated in each of the designated time intervals. The values were mean ± SE of three independent experiments. D, E. Western blot analysis of the AURKA, pAURKA(T288), HIF1α, NFκB p50, NFκB p65, Total Akt, pAkt(S473), p53 and Gadd45α expressions in SiHa and SiHa/RR cells exposed to acute radiation dose of 10Gy. β actin was used as loading control. Experiments were done in triplicate. F. Network based analysis of proteins to study their interactions with AURKA; showing close interactions among these proteins which have altered expression status in SiHa/RR. **$p < 0.001$.

Citation: Salini Das, Dilip Kumar Ray, Elizabeth Mahapatra, Souvick Biswas, Debomita Sengupta, Madhumita Roy, Sutapa Mukherjee. AURKA/NFκB Axis: A Key Determinant of Radioresistance in Cervical Squamous Carcinoma Cells. Archives of Clinical and Biomedical Research 6 (2022): 707-721.

Das S et al., Arch Clin Biomed Res 2022
DOI:10.26502/acbr.50170282

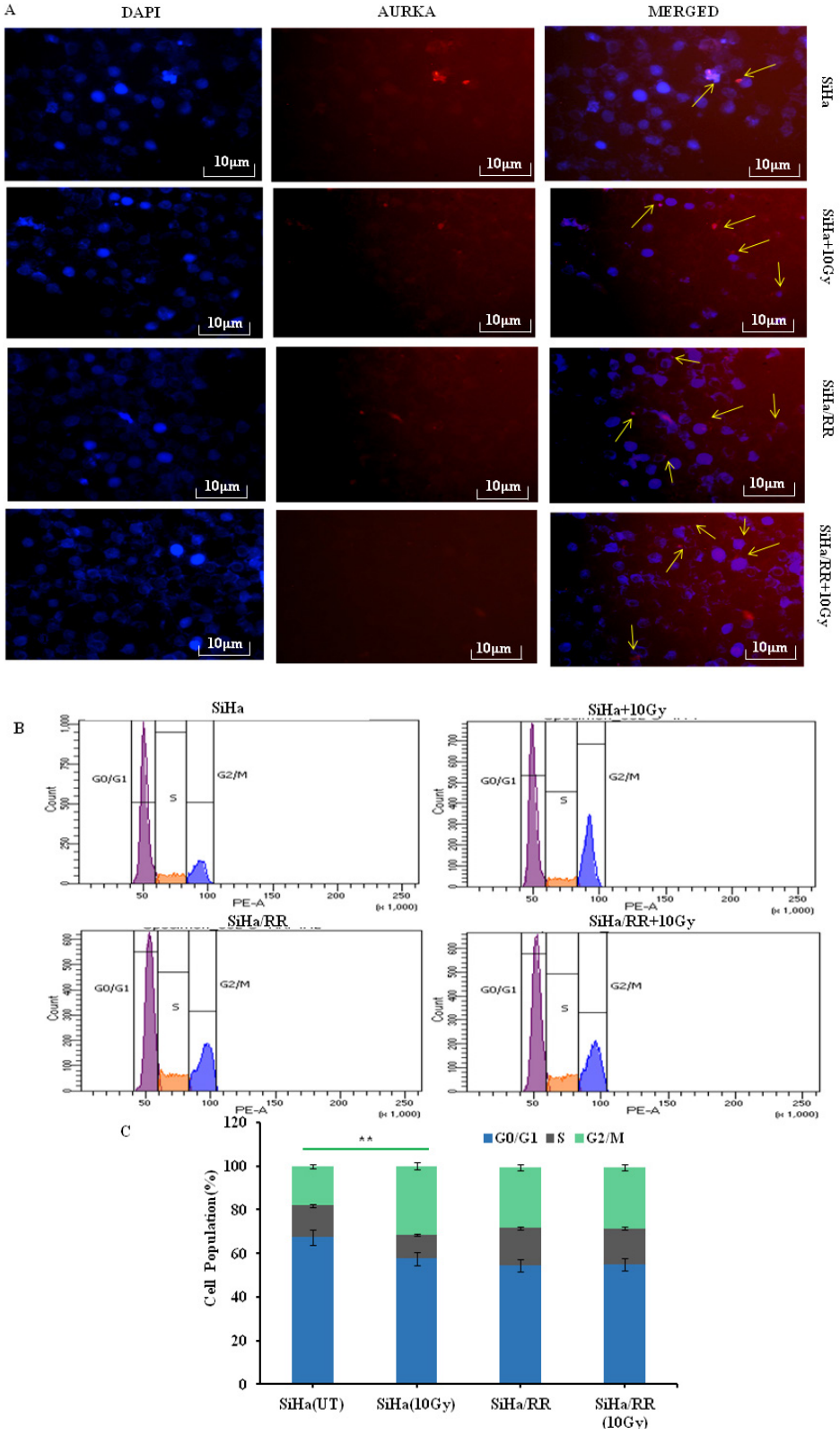

Figure 2: Acquired radioresistant subline SiHa/RR escapes G2/M arrest by virtue of elevated AURKA level: A. Centrosomal and nuclear localization (yellow arrows) of AURKA in SiHa and SiHa/RR cells. Immunostained cells showing altered localization of AURKA in SiHa/RR in the presence and absence of 10Gy radiations. B. Cell cycle distribution of radioresistant (SiHa/RR) and radiosensitive SiHa, exposed to acute dose of 10Gy radiation. Distribution of cells at different phases was measured by flow cytometry succeeding propidium iodide (PI) staining. C. Frequency distribution of cells at different phases of cell cycle shows unaltered G2/M cell population in SiHa/RR even after acute radiation exposure to 10Gy. Data are represented as Mean ± SD of three independent experiments. **p< 0.001.

Citation: Salini Das, Dilip Kumar Ray, Elizabeth Mahapatra, Souvick Biswas, Debomita Sengupta, Madhumita Roy, Sutapa Mukherjee. AURKA/NFκB Axis: A Key Determinant of Radioresistance in Cervical Squamous Carcinoma Cells. Archives of Clinical and Biomedical Research 6 (2022): 707-721.

Das S et al., Arch Clin Biomed Res 2022
DOI:10.26502/acbr.50170282

similar trend of reduced G2/M population (as that for SiHa/RR) in the transfected SiHa cells; even after acute exposure dose of 10Gy radiation (Figure 3D and E). Contributory role of AURKA in rendering radioresistance was further assessed by exposing both SiHa and AURKA-overexpressed SiHa to 2, 4, 6, 8, 10Gy of radiation and corresponding MTT assay were performed for understanding the cell viability. Results indicated higher viability (%) in AURKA-overexpressed SiHa cells compared to parental SiHa; suggesting an acquired radioresistant phenotype in AURKA-overexpressed cells (Figure 3F). Immunofluorescence staining showed distinct nuclear localization of NFκB (p50 & p65) subunits in the AURKA-transfected cells. This finding validated the previous observation regarding predominance of nuclear localization of NFκB in SiHa/RR cells (Figure 3 G).

Inhibition of AURKA Reinstates Radiosensitivity by Reversing Radioadaptive Response in SiHa/RR Cells

To establish the mediatory role of AURKA in restricting radiation induced cell killing, both SiHa and SiHa/RR cells were pretreated with Aurora A Inhibitor I (0.01 μM) for 6h , subjected to acute dose of irradiation with 10Gy and subsequently incubated for additional 6h. It was obvious from the result that the pretreatment with AURKA inhibitor increased the radiosensitivity of SiHa/RR as evident from the result (Figure 4A) with decreased percentage of viable cells. This result highlighted the role of AURKA in manifesting radioresistance in SiHa/RR cells. Western blot results also revealed diminished expression of AURKA upon AKI treatment. To explore the consequence of AURKA inhibition, expression of its downstream effectors NFκB (p50 and p65) was re-performed using nuclear extract of SiHa/RR cells. The expression of NFκB was effectively reduced as a consequence of AURKA inhibition (Figure 4B). These observations clearly highlighted that AURKA inhibition is correlated with hindered nuclear translocation of NFκB. Since Oct4 and MMP9 are the downstream effectors of NFκB, western blot analysis was further carried out to validate the findings. Upregulated expression of stemness marker Oct4 in SiHa/RR cells were significantly reduced upon pretreatment with AURKA inhibitor. Similar trend in expression pattern of metastatic marker MMP9 was documented from the result (Figure 4C). Immunofluorescence study in presence of AKI showed diminished expressions of both NFκB p65 and p50 subunits, which further justified the involvement of AURKA in the induction of nuclear localization of NFκB. This observation was in agreement with the western blot study (Figure 4D and E). It was next felt obvious to check whether inhibition of AURKA, ultimately lead to radiation induced cell killing by apoptotic pathway. Both SiHa and SiHa/RR were either/or pretreated with AKI, followed by radiation exposure (10Gy) prior to TUNEL assay. Untreated cells showed a relatively lesser apoptotic nucleus, whereas upon exposure to 10Gy irradiation, SiHa exhibited characteristic morphological features of apoptotic cells when observed under fluorescent microscope. Some of the notable apoptotic features with higher frequencies of fragmented nuclei were found in SiHa (Figure 4F). SiHa/RR on the contrary failed to undergo apoptosis upon 10Gy irradiation. Nonetheless treatment of SiHa/RR with Aurora A Inhibitor I prior to acute shot of irradiation sensitized cells to undergo radiation induced apoptosis; confirming the implication of AURKA in developing radioadaptive response to escape apoptosis (Figure 4F).

AURKA Inhibition Lessened the Wound Healing and Sphere Forming Ability of SiHa/RR Cells

To check whether SiHa/RR cells have developed the traits of increased cell migration and invasion ability, 2D scratch assay was performed. Wound healing assay or scratch assay revealed that SiHa/RR had the ability of remarkably faster closure rate of wound area compared to SiHa (Figure 5A). Cell migration of SiHa/RR cells was found to be increased by 60%, in comparison to control SiHa (Figure 5B). Prior exposure to AURKA inhibitor remarkably and distinguishably prevented the wound closure ability of SiHa/RR cells by obstructing its migratory capacity. This result clearly advocated the involvement of elevated expression of AURKA in mediating radioresistant phenotype by increasing migratory potential of the SiHa/RR cells. These interesting findings also justified further about the attribution of AURKA in development of radioresistance by inducing stemness and metastasis in radioresistant subline SiHa/RR. Sphere forming assay revealed development of nonadherent spherical clusters of cells particularly in SiHa/RR; one week after cell seeding in anchorage independent condition. These results justified the previous findings of better migration and invasion property in radioresistant SiHa/RR cells. To further establish the possible involvement of AURKA in acquirement of radioadaptive response, by increased migration and proliferation potential, both SiHa and SiHa/RR were treated with Aurora A Inhibitor I at a dose of 0.01 μM. Sphere forming ability of both SiHa and SiHa/RR was reduced significantly after 36h (Figure 5C). Fold increase in sphere area was calculated using FIJI software. The graphical result (Figure 5D) clearly corroborated with the microscopic findings. Sphere forming ability is considered as a phenotype of acquirement of tumorigenicity and stemness feature. Therefore, AKI mediated reduction in sphere formation as obtained from the results of reduced sphere area specified that inhibition of AURKA can sufficiently reverse the acquired radioadaptive features of SiHa/RR.

Das S et al., Arch Clin Biomed Res 2022
DOI:10.26502/acbr.50170282

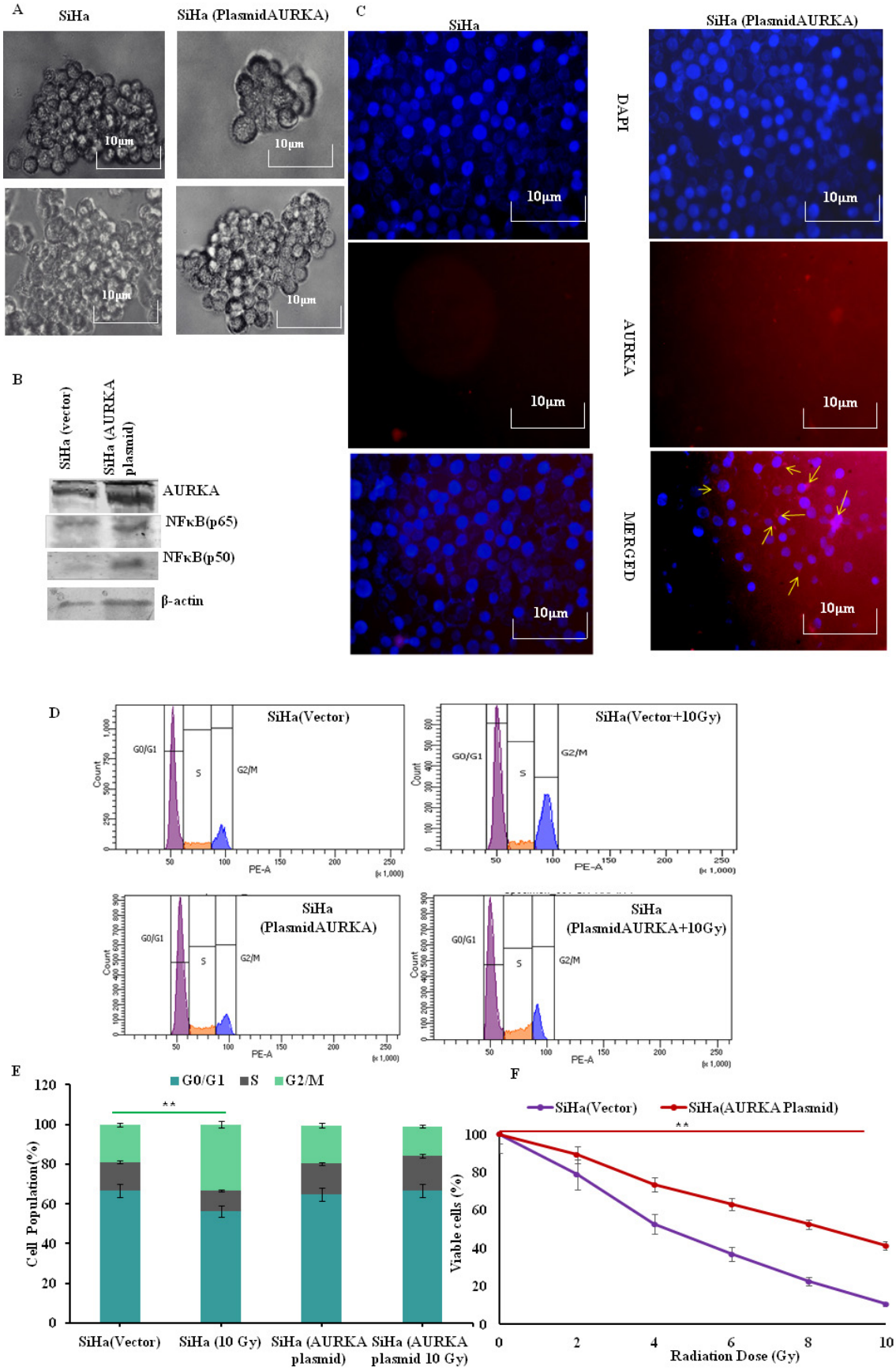

Citation: Salini Das, Dilip Kumar Ray, Elizabeth Mahapatra, Souvick Biswas, Debomita Sengupta, Madhumita Roy, Sutapa Mukherjee. AURKA/ NFκB Axis: A Key Determinant of Radioresistance in Cervical Squamous Carcinoma Cells. Archives of Clinical and Biomedical Research 6 (2022): 707-721.

Das S et al., Arch Clin Biomed Res 2022
DOI:10.26502/acbr.50170282

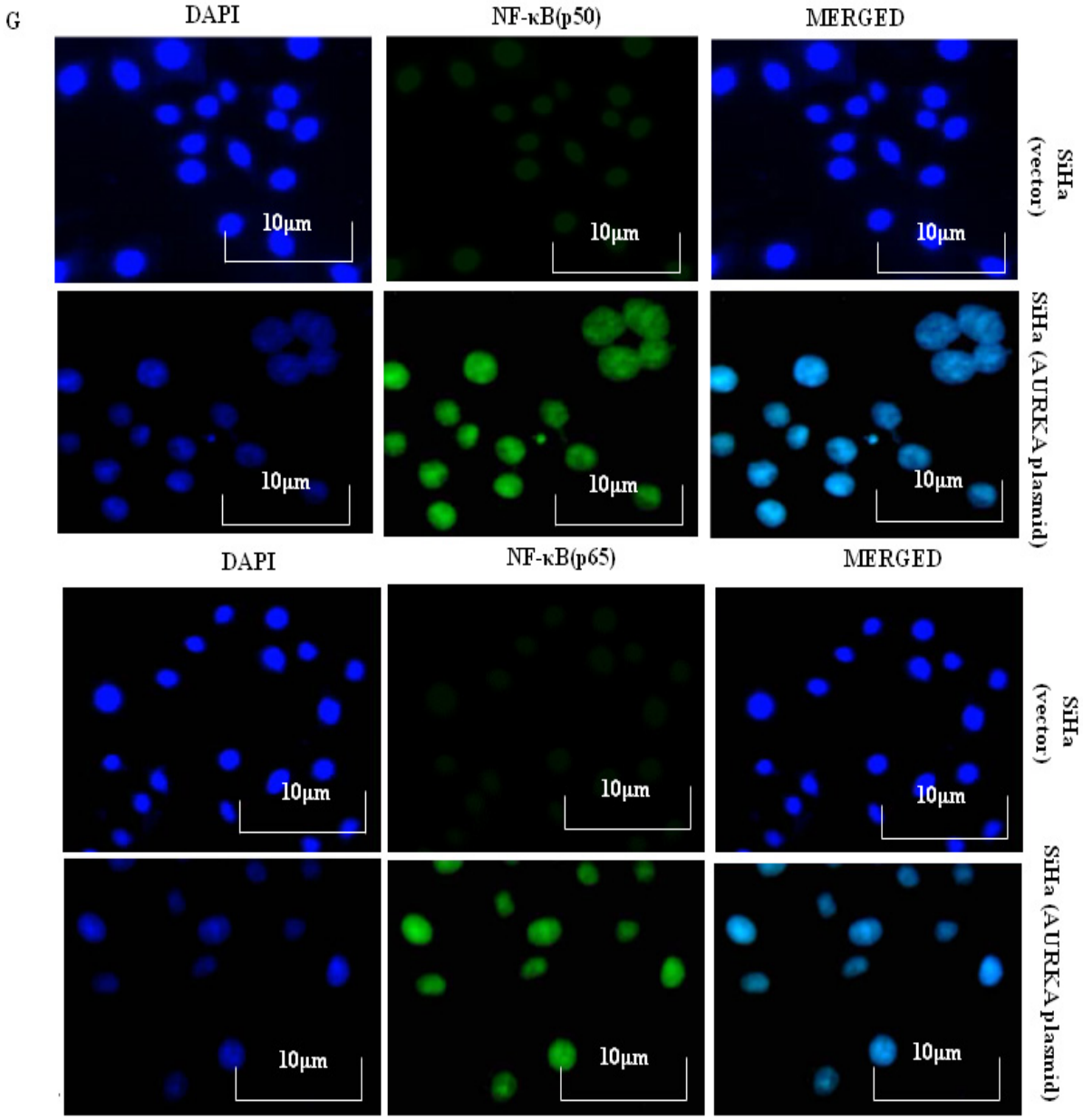

Figure 3: Involvement of AURKA in imparting radioresistant phenotype was confirmed by Ectopic overexpression of AURKA in parental SiHa: A. Parental SiHa with ectopically overexpressed AURKA shows better sphere forming abilities with enlarged sphere area compared to vector control SiHa. B. Upregulated expression of AURKA was obvious in AURKA overexpressed cells alongside elevated expression of its downstream signaling factor NFκB (p50/p65) as observed from Western blot analysis. β-actin was used to ensure equal protein loading. C. Immunofluorescence study confirming overexpression of AURKA in plasmid transfected cells (yellow arrows). Each representative image was captured at 400X, scale bar: 10 µm. D. Cell cycle phase specific distribution of SiHa (vector control vs AURKA transfected); showing radiation induced G2/M arrest in SiHa (Vector control) although progression towards G2/M was evident in AURKA overexpressed SiHa. Results are representative of three independent experiments. E. Graphical representation showing cell cycle phase specific distribution pattern of SiHa (% of cells) in vector control vs AURKA transfected cells. Each experiment was performed in triplicates and the values obtained are Mean ± SD with significance level **p< 0.001. F. Radioresistant phenotype of AURKA overexpressed SiHa was further confirmed by calculating cell viability (%), obtained from the findings of MTT assay. Experiments were done in triplicate. Values obtained are Mean ±SD with **p <0.001 G. AURKA overexpressed cells facilitated increased nuclear localization of NF-κB (p50) and p65 as evident from Immunofluorescence study using specific antibodies against p50 and p65 subunits (Magnification: 400X).

Das S et al., Arch Clin Biomed Res 2022
DOI:10.26502/acbr.50170282

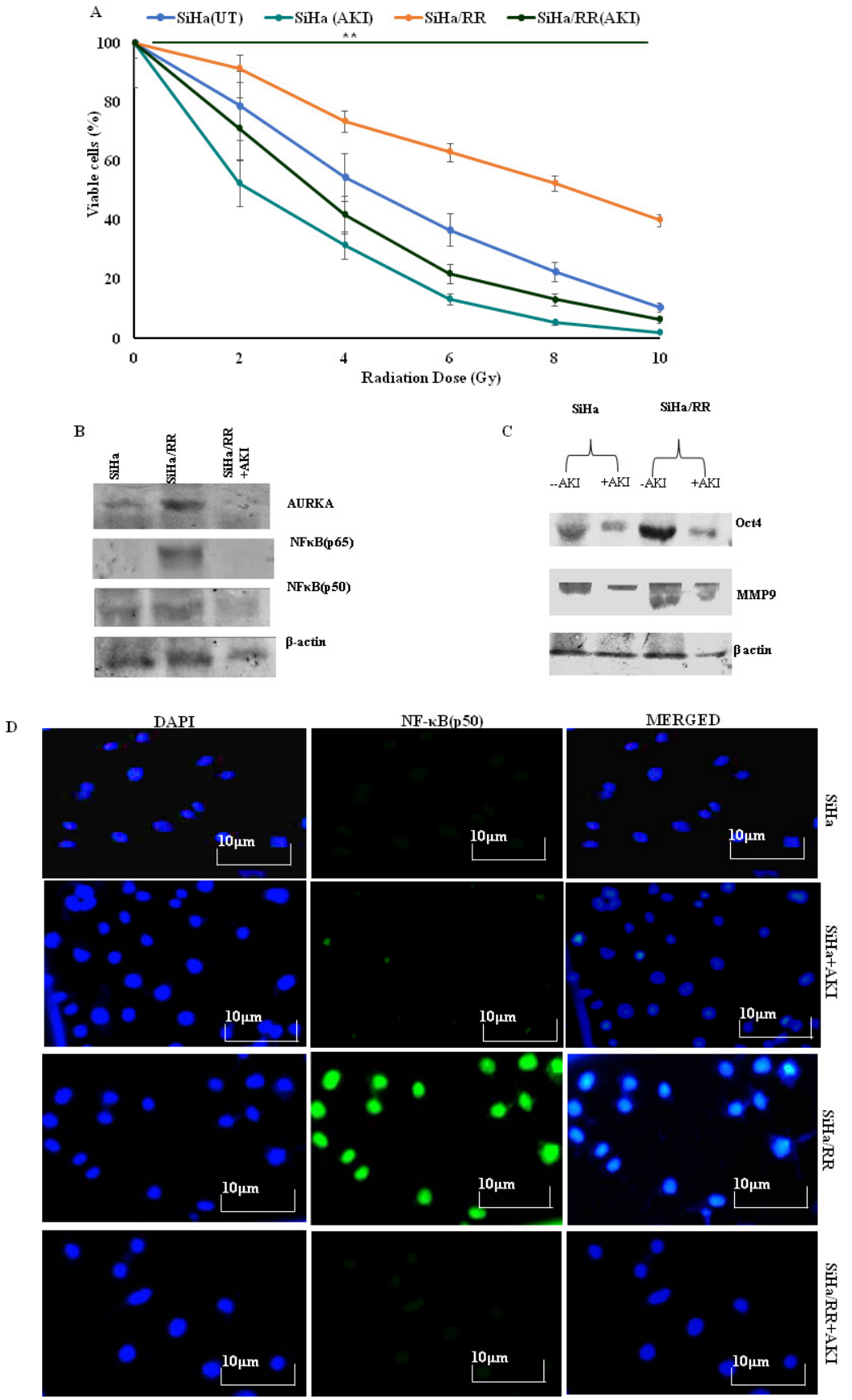

Citation: Salini Das, Dilip Kumar Ray, Elizabeth Mahapatra, Souvick Biswas, Debomita Sengupta, Madhumita Roy, Sutapa Mukherjee. AURKA/ NFκB Axis: A Key Determinant of Radioresistance in Cervical Squamous Carcinoma Cells. Archives of Clinical and Biomedical Research 6 (2022): 707-721.

Das S et al., Arch Clin Biomed Res 2022
DOI:10.26502/acbr.50170282

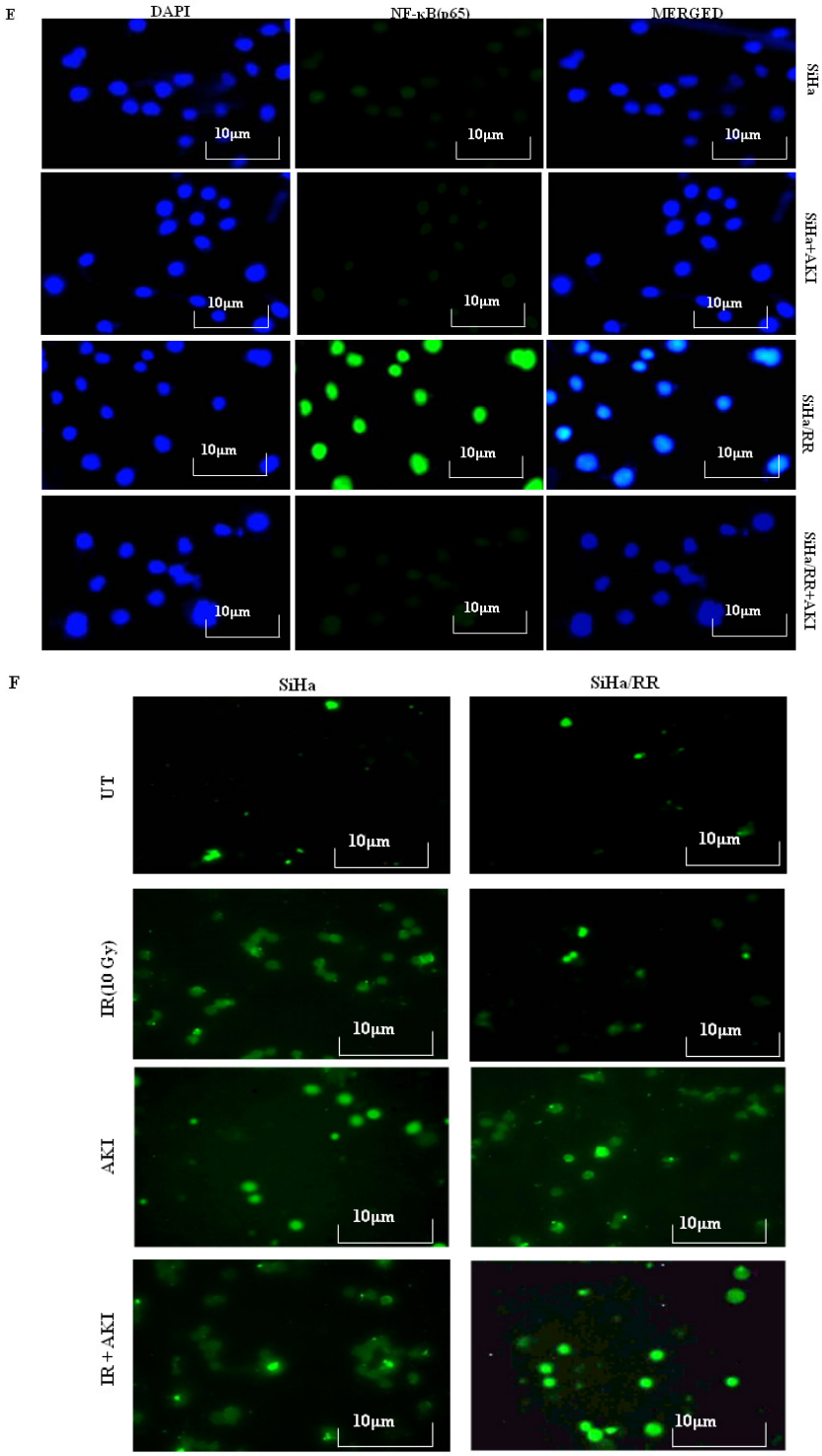

Figure 4: AURKA inhibition impedes NFκB signaling with concomitant prevention of aggressive behaviour of radioresistant cells and induction of apoptosis: A. SiHa and SiHa/RR cells were either/or pretreated with Aurora Kinase A Inhibitor I (AKI; 0.01 µM) for 6h followed by exposed to irradiation with an acute dose of 10Gy. Cell viability (%) was calculated based on the results obtained from MTT assay. Values are mean ±SD of three independent experimnents. B. Western blot data showing reduction in the expressions of AURKA, NF-κB p50 and p65 in radioresistant SiHa/RR as a result of AURKA inhibition. C. Differential expression patterns of OCT4 and MMP9 proteins in SiHa and SiHa/RR cells exposed to10Gy irradiation, prior to treatment with or without AKI; displayed diminished expressions of these EMT markers in SiHa/RR owing to AURKA inhibition. D. Immunofluorescent Staining of AKI pretreated SiHa/RR cells efficiently brought down nuclear localization of p50 as well as p65 (Figure E). The results are representative images of three independent experiments with a magnification of 400X; scale bar: 10 µm F. Acquired radioresistance was apparent in SiHa/RR cells where apoptotic ability was minimal upon 10Gy radiation (Figure4F; right panel) comparable with untreated (UT) cells. Pretreatment of SiHa/RR cells with AKI restored radiosensitivity as increased frequency of apoptotic cells were noticeable in TUNEL labelled (FITC) SiHa/RR cells. SiHa being radiosensitive cells was taken as a reference control.

Citation: Salini Das, Dilip Kumar Ray, Elizabeth Mahapatra, Souvick Biswas, Debomita Sengupta, Madhumita Roy, Sutapa Mukherjee. AURKA/NFκB Axis: A Key Determinant of Radioresistance in Cervical Squamous Carcinoma Cells. Archives of Clinical and Biomedical Research 6 (2022): 707-721.

Das S et al., Arch Clin Biomed Res 2022
DOI:10.26502/acbr.50170282

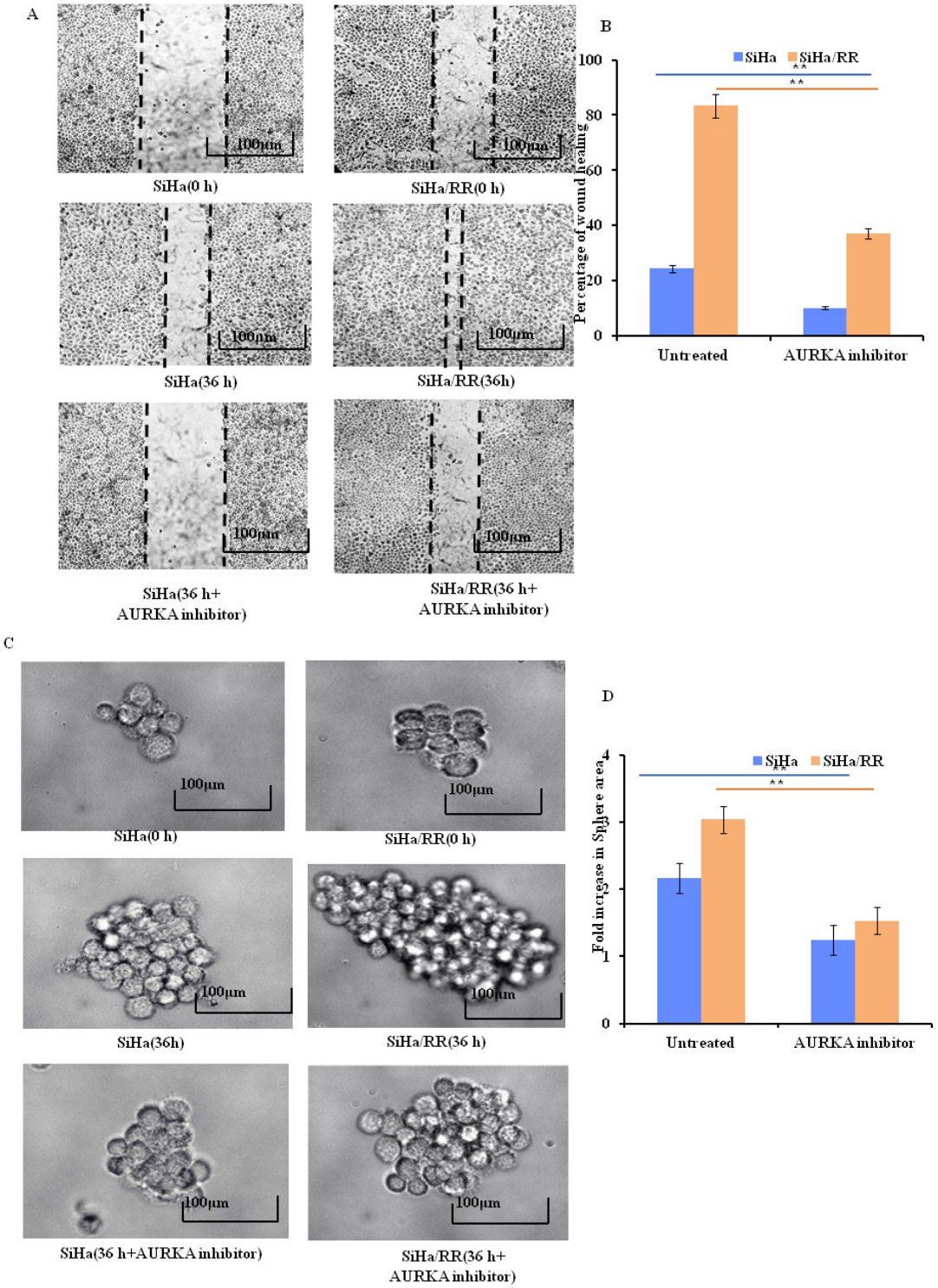

Figure 5: "AURKA inhibition reduces adaptive metastatic potential of SiHa/RR: A. SiHa/RR showed decreased rate of wound closure ability upon treatment with AKI compared to untreated cells. B. Graphical representation of percentage of wound closure of SiHa and SiHa/RR in the presence and absence of AKI after 36h of scratch formation. Healing of scratch area of corresponding groups was quantitated by calculating the wound area. The values represented Mean ± SD of three independent experiments. $^{**}p<0.001$ is significant, compared to respective controls. C. SiHa and SiHa/RR cells were treated without (control) or with AKI (0.01 µM) for 36h. Formation of spheres in all the treatment groups was observed under an Inverted Microscope (Olympus). Images were captured at 100X; scale bar 100 µm. Sphere forming ability of SiHa/RR was significantly reduced upon treatment with AKI. D. Relative fold changes of sphere area were calculated and as depicted from the graphical data, disclosed the downregulated growth of sphere area in SiHa/RR in the presence of AKI. Representative plots depicted restrained sphere formation upon AKI treatment in SiHa and SiHa/RR. All the experiments were repeated thrice and values were taken as Mean ± SD, $^{**}p< 0.001$."

Citation: Salini Das, Dilip Kumar Ray, Elizabeth Mahapatra, Souvick Biswas, Debomita Sengupta, Madhumita Roy, Sutapa Mukherjee. AURKA/ NFκB Axis: A Key Determinant of Radioresistance in Cervical Squamous Carcinoma Cells. Archives of Clinical and Biomedical Research 6 (2022): 707-721.

Das S et al., Arch Clin Biomed Res 2022
DOI:10.26502/acbr.50170282

Discussion

The primary purpose of this study was to characterize radioresistant cells to investigate the involvement of AURKA in imparting radioresistant phenotype in cervical cancer cells. Since the invasive carcinoma of cervix occurs at the squamo-columnar junction, cervical squamous carcinoma cell line (SiHa) was used for the study. Developing a radioresistant subline SiHa/RR from parental SiHa was accomplished by fractionated irradiation. Chronic irradiation for a cumulative period of 6 months finally contributed in acquirement of radioadaptive alterations in SiHa/RR; particularly in morphological characteristics, which showed increased N/C ratio. The significant reduction in doubling time to 24 h in SiHa/RR from 33 h in parental SiHa clearly gave an indication of faster proliferation rate. To furthrer explore the potential of radioresistant subline SiHa/RR in overcoming radiation induced cell killing, cell viability assay was performed. The result depicted noticeably high viability rate in SiHa/RR even after challenging with 10Gy radiation. This outrageous cell proliferative potential made it pertinent to check the expression patterns of AURKA, an important enzyme of G2-M phase. Increased proliferative potential of radioresistant subline was in coherence with the expressional status of AURKA, the expression of which was appreciably high in radioresistant subline SiHa/RR and remained unaltered even after exposure to acute radiation of 10Gy. Moreover, upregulated expression of upstream regulator (HIF1α) and downstream regulator NFκB (p50/65) of AURKA further strengthened the notion of AURKA mediated acquired radioresistance in SiHa/RR cells. Since phosphorylation of Akt is reported to be mediated by AURKA [22], therefore, the expressions of Akt and phospho Akt (S473) were examined furthermore. Akt and phospho Akt (S473) were found to be overexpressed in SiHa/RR. Contrarily, protein levels of DNA damage markers like p53, Gadd45α were downregulated in SiHa/RR subline. Studies have documented that AURKA lowers the expressions of p53 by regulatory phosphorylation at S215 and S315 residues, which in turn facilitates p53 degradation via MDM2 mediated ubiquitination [23]. Downregulated expression of p53 and GADD45α as evidenced from the present findings possibly promoted G2/M progression as both the molecules cause cell cycle arrest in response to radiation induced DNA damage [24, 25]. String interaction results indicated interplay of signaling molecules of AURKA pathway in SiHa/RR. AURKA was found to be strongly interacted with p53, Gadd45α, Akt and NFκB. Considering the functional role of AURKA as G2-M regulator, it was felt curious to find out whether any distinguishable difference in cell cycle pattern in SiHa/RR occurs as opposed to SiHa. Since the radiation efficacy depends on the phases of cell cycle, the strategy of radioresistant cells involve adjusting the cell cycle pattern in response to irradiation [26]. The increased G2/M population in SiHa cells is indicative to its radiosensitivity, as radiation cause G2/M arrest for effective killing of cells. Conversely, SiHa/RR showed reduced G2/M population emphasizing the potential of overcoming the G2/M arrest, which enabled SiHa/RR cells to continue cell cycle progression. These observations supported the previous findings where AURKA was shown to exert a key role in acquisition of radioresistance. To further validate the potential contribution of this kinase in radioresistance in SiHa/RR, ectopic overexpression of AURKA and subsequent alteration in the radiosensitivity was assessed in parental SiHa. AURKA transfected SiHa showed similar trends of radioresistant phenotype as that of SiHa/RR, not only in terms of improved viability but also in better sphere forming ability. The principal mechanism in imparting radioresistance mediated by AURKA was activation of prosurvival pathway via facilitating nuclear localization of NFκB as observed earlier in SiHa/RR as well as in SiHa transfected with AURKA plasmid. The enhanced expression of NFκB in the nuclear fraction strengthens the notion of AURKA mediated activation of NFκB in AURKA-transfected SiHa and corroborated with the findings for SiHa/RR. These observations were in agreement with some of the previous findings where AURKA with other downstream signaling axis showed significant contribution in acquisition of radioresistance in cancer [27-34]. Overexpression of AURKA coincided with the acquired features of SiHa/RR which justified the hypothesis of involvement of AURKA as a mediator to acquire radioadaptive response in cervical cancer cells for the attainment of radioresistance by promoting nuclear translocation of NFκB. These findings prompted to further check whether any changes in cellular phenotype occurs upon AURKA inhibition. To address the problem, cell viability study was performed in presence and absence of AURKA inhibitor. SiHa/RR while treatment with AKI showed a notable reduction in percentage of viable cells compared to the untreated cells. Apoptotic study further affirmed lesser responsiveness of SiHa/RR towards apoptosis as revealed from the results obtained from TUNEL assay. Increased radiosensitivity was further documented by increasing the radiation induced apoptosis potential upon treatment with AKI in both SiHa and SiHa/RR. These findings explained increased radiosensitizing potential upon AURKA inhibition in SiHa/RR cells. This observation was in agreement with the previous studies which emphasized the likelihood of AURKA in attainment of radioadaptive alterations in SiHa/RR. [35]. Hyper-proliferative potential of SiHa/RR aided in increased migration and invasion capabilities as evident from the result of wound healing assay where SiHa/RR filled the gap at a much faster rate compared to SiHa. The 3D spheroid forming ability was increased in SiHa/RR as measured by the increased sphere area. The subsequent reduction in wound healing property and sphere forming capacity in SiHa/RR upon treatment with AKI made the possibility stronger that AURKA helped in the induction of stemness and metastasis in the radioresistant cells. Further experimentation was

conducted to check the expressions of Oct4 and MMP9; two known markers of stemness and EMT; which are known downstream effector of NFκB [36,37]. Western blot analysis was performed in presence and absence of AKI for venturing the role of AURKA in the induction of EMT and stemness in SiHa/RR. The result indicated AURKA mediated acquisition of radioresistance with development of more mesenchymal like phenotype along with increased potential of invasion and migration in SiHa/RR cells. Both of these molecules were overexpressed in SiHa/RR but got downregulated upon administration of AKI. These findings further reinforced the experimental outcome of other investigators which justified epithelial-to mesenchymal transition (EMT) as notable phenotypic and molecular alterations [38-40].

Conclusions

Accumulation of radioadaptive response within cells owing to chronic administration of incremental doses of radiation was revealed from the present findings where chronic irradiation generated several survival approaches. This elevated survival capability of SiHa/RR was achieved by tuning the existing molecular scenario such as triggering the expression of prosurvival molecules and overcoming necessary arrest to minimize the chances of apoptotic stimulation. Interestingly these alterations generated in course of radioresistance coincide with majority of the functional activities of AURKA including cell proliferation, migration, invasion, epithelial-mesenchymal transition (EMT) and maintenance of cancer stem cell (CSC) behaviors and led to anticipate AURKA as one of the prime mediators of radioresistance in cancer. This work therefore provides an access to a new horizon of further investigations to establish AURKA not only as a biomarker but also an essential therapeutic target to combat radioresistance.

Acknowledgements

The Authors are indebted to Council of Scientific and Industrial Research (CSIR), New Delhi, Govt. of India for providing fellowship and contingency fund for the project. The authors convey sincere thanks to Director Chittaranjan National Cancer Institute, Kolkata, INDIA for providing infrastructural facilities required for the work. The authors are grateful to Radiation unit, CNCI for their help in irradiation protocol.

Conflicts of Interest

The authors declare no conflict of interest.

References

1. Arbyn M, Weiderpass E, Bruni L, et al. Estimates of incidence and mortality of cervical cancer in 2018: a worldwide analysis. The Lancet. Global health 8 (2020): e191–e203.
2. Sung H, Ferlay J, Siegel RL, et al. Global cancer statistics 2020: GLOBOCAN estimates of incidence and mortality worldwide for 36 cancers in 185 countries. CA: a cancer journal for clinicians 71(2021): 209-249.
3. Burmeister CA, Khan SF, Schäfer G, et al. Cervical cancer therapies: Current challenges and future perspectives. Tumour Virus Res 13 (2022): 200238.
4. Tyagi A, Vishnoi K, Kaur H, et al. Cervical cancer stem cells manifest radioresistance: Association with upregulated AP-1 activity. Scientific reports 7 (2017):1-14.
5. Randall LM, Walker AJ, Jia AY, et al. Expanding Our Impact in Cervical Cancer Treatment: Novel Immunotherapies, Radiation Innovations, and Consideration of Rare Histologies. Am Soc Clin Oncol Educ Book 41 (2021): 252263.
6. Yang J, Cai H, Xiao ZX, et al. Effect of radiotherapy on the survival of cervical cancer patients: An analysis based on SEER database. Medicine (Baltimore) 98 (2019): 16421.
7. Denny L. Cervical cancer: prevention and treatment. Discov Med 14 (2012): 125-131.
8. Vora C, Gupta S. Targeted therapy in cervical cancer. ESMO Open 3 (2019): 000462.
9. Pawlik TM, Keyomarsi K. Role of cell cycle in mediating sensitivity to radiotherapy. International Journal of Radiation Oncology Biology Physics 59 (2004): 928-942.
10. Dillon MT, Good JS, Harrington KJ. Selective targeting of the G2/M cell cycle checkpoint to improve the therapeutic index of radiotherapy. Clinical oncology 26 (2014): 257-265.
11. de Jong Y, Ingola M, Briaire-de Bruijn IH, et al. Radiotherapy resistance in chondrosarcoma cells; a possible correlation with alterations in cell cycle related genes. Clinical sarcoma research 9 (2901): 1-11.
12. Liu X, Zhang Y, Wu S, et al. Palmatine induces G2/M phase arrest and mitochondrial-associated pathway apoptosis in colon cancer cells by targeting AURKA. Biochemical pharmacology 175 (2020): 113933.
13. Nikonova AS, Astsaturov I, Serebriiskii IG, et al. Aurora A kinase (AURKA) in normal and pathological cell division. Cellular and Molecular Life Sciences 70 (2013): 661-687.
14. Das S, Mahapatra E, Biswas S, et al. Emerging Role of Aurora A in Radioresistance: A Comprehensive Review. EMJ 9 (2021): 81-90.
15. Biswas S, Mahapatra E, Ghosh A, et al. Curcumin rescues doxorubicin responsiveness via regulating Aurora a signaling network in breast cancer cells. Asian Pac J Cancer Prev 22 (2021): 957-970.

Das S et al., Arch Clin Biomed Res 2022
DOI:10.26502/acbr.50170282

16. Lee SY, Jeong EK, Ju MK, et al. Induction of metastasis, cancer stem cell phenotype, and oncogenic metabolism in cancer cells by ionizing radiation. Mol Cancer 16 (2017): 10.

17. Liu F, Zhang Y, Dong Y, et al. Knockdown of AURKA sensitizes the efficacy of radiation in human colorectal cancer. Life Sciences 271 (2021): 119148.

18. Oh ET, Byun MS, Lee H, et al. Aurora-a contributes to radioresistance by increasing NF-kappaB DNA binding. Radiat Res 174 (2010): 26573.

19. Sarkar R, Mukherjee S, Roy M. Targeting heat shock proteins by phenethyl isothiocyanate results in cell-cycle arrest and apoptosis of human breast cancer cells. Nutr Cancer 65 (2013): 480-493.

20. Biswas S, Mahapatra E, Roy M, et al. PEITC by regulating Aurora Kinase A reverses chemoresistance in breast cancer cells. Indian Journal of Biochemistry and Biophysics (IJBB) 57 (2020): 167-177.

21. Foty R. A simple hanging drop cell culture protocol for generation of 3D spheroids. J Vis Exp 51 (2011): 2720.

22. Wu J, Cheng Z, Xu X, et al. Aurora-A Induces Chemoresistance Through Activation of the AKT/mTOR Pathway in Endometrial Cancer. Front Oncol 9 (2019): 422.

23. Sasai K, Treekitkarnmongkol W, Kai K, et al. Functional Significance of Aurora Kinases-p53 Protein Family Interactions in Cancer. Front Oncol 6 (2016): 247.

24. Otani K, Naito Y, Sakaguchi Y, et al. Cell-cycle-controlled radiation therapy was effective for treating a murine malignant melanoma cell line in vitro and in vivo. Scientific reports 6 (2016): 1-8.

25. Singh SK, Banerjee S, Acosta EP, et al. Resveratrol induces cell cycle arrest and apoptosis with docetaxel in prostate cancer cells via a p53/ p21WAF1/CIP1 and p27KIP1 pathway. Oncotarget 8(2017): 17216-17228.

26. Pajonk F, Vlashi E, McBride WH. Radiation resistance of cancer stem cells: the 4 R's of radiobiology revisited. Stem Cells 4 (2010): 639-648.

27. Janeček M, Rossmann M, Sharma P, et al. Allosteric modulation of AURKA kinase activity by a smallmolecule inhibitor of its proteinprotein interaction with TPX2. Scientific reports 6 (2016): 1-12.

28. Du R, Huang C, Liu K, et al. Targeting AURKA in Cancer: molecular mechanisms and opportunities for Cancer therapy. Molecular Cancer 20 (2021): 1- 27.

29. Miralaei N, Majd A, Ghaedi K, et al. Integrated pan-cancer of AURKA expression and drug sensitivity analysis reveals increased expression of AURKA is responsible for drug resistance. Cancer Medicine 10 (2021): 64286441.

30. Liu F, Zhang Y, Dong Y, et al. Knockdown of AURKA sensitizes the efficacy of radiation in human colorectal cancer. Life Sciences 271 (2021): 119148.

31. Shen ZT, Chen Y, Huang GC, et al. Aurora-a confers radioresistance in human hepatocellular carcinoma by activating NF-κB signaling pathway. BMC Cancer 19 (2019): 1075

32. Liu JB, Hu L, Yang Z, et al. Aurora-A/NF-κB signaling is associated with radio-resistance in human lung adenocarcinoma. Anticancer Res 39 (2019): 5991-5998.

33. Guan Z, Wang XR, Zhu XF, et al. Aurora-A, a negative prognostic marker, increases migration and decreases radiosensitivity in cancer cells. Cancer Res 67 (2007): 10436-10444.

34. Sun H, Wang Y, Wang Z, et al. Aurora-A controls cancer cell radio- and chemoresistance via ATM/Chk2-mediated DNA repair networks. BiochimBiophys Acta 1843 (2014): 934-944.

35. Tahmasebi-Birgani MJ, Teimoori A, Ghadiri A, et al. Fractionated radiotherapy might induce epithelial-mesenchymal transition and radioresistance in a cellular context manner. J Cell Biochem 120 (2018): 8601-8610.

36. Fan X, Zhou J, Bi X, et al. L-theanine suppresses the metastasis of prostate cancer by downregulating MMP9 and Snail. J NutrBiochem 89 (2021): 108556.

37. Jin Y, Xu K, Chen Q, et al. Simvastatin inhibits the development of radioresistant esophageal cancer cells by increasing the radiosensitivity and reversing EMT process via the PTEN-PI3K/AKT pathway. Exp Cell Res 362 (2018): 362369.

38. Konge J, Leteurtre F, Goislard M, et al. Breast cancer stem cell-like cells generated during TGFβ-induced EMT are radioresistant. Oncotarget 9 (2018): 23519-23531.

39. Zhou S, Zhang M, Zhou C, et al. The role of epithelialmesenchymal transition in regulating radioresistance. Crit Rev Oncol Hematol 150 (2020): 102961.

40. Steinbichler TB, Alshaimaa A, Maria MV, et al. Epithelial-mesenchymal crosstalk induces radioresistance in HNSCC cells. Oncotarget 9 (2017): 3641-3652.

Citation: Salini Das, Dilip Kumar Ray, Elizabeth Mahapatra, Souvick Biswas, Debomita Sengupta, Madhumita Roy, Sutapa Mukherjee. AURKA/NFκB Axis: A Key Determinant of Radioresistance in Cervical Squamous Carcinoma Cells. Archives of Clinical and Biomedical Research 6 (2022): 707-721.